

# Paleohistology of the intercentra of North American metoposaurids from the Upper Triassic of Petrified Forest National Park (Arizona, USA) with implications for the taxonomy and ontogeny of the group (#14552)

1

First submission

Please read the **Important notes** below, the **Review guidance** on page 2 and our **Standout reviewing tips** on page 3. When ready [submit online](#). The manuscript starts on page 4.

## Important notes

### Editor and deadline

Andrew Farke / 5 Jan 2017

### Files

8 Figure file(s)  
2 Table file(s)

Please visit the overview page to [download and review](#) the files not included in this review PDF.

### Declarations

No notable declarations are present



Please read in full before you begin

## How to review






When ready [submit your review online](#). The review form is divided into 5 sections. Please consider these when composing your review:

- 1. BASIC REPORTING**
- 2. EXPERIMENTAL DESIGN**
- 3. VALIDITY OF THE FINDINGS**
4. General comments
5. Confidential notes to the editor

 You can also annotate this PDF and upload it as part of your review

To finish, enter your editorial recommendation (accept, revise or reject) and submit.

### BASIC REPORTING

-  Clear, unambiguous, professional English language used throughout.
-  Intro & background to show context. Literature well referenced & relevant.
-  Structure conforms to [PeerJ standards](#), discipline norm, or improved for clarity.
-  Figures are relevant, high quality, well labelled & described.
-  Raw data supplied (see [PeerJ policy](#)).

### EXPERIMENTAL DESIGN

-  Original primary research within [Scope of the journal](#).
-  Research question well defined, relevant & meaningful. It is stated how the research fills an identified knowledge gap.
-  Rigorous investigation performed to a high technical & ethical standard.
-  Methods described with sufficient detail & information to replicate.

### VALIDITY OF THE FINDINGS

-  Impact and novelty not assessed. Negative/inconclusive results accepted. *Meaningful* replication encouraged where rationale & benefit to literature is clearly stated.
-  Data is robust, statistically sound, & controlled.
-  Conclusions are well stated, linked to original research question & limited to supporting results.
-  Speculation is welcome, but should be identified as such.

The above is the editorial criteria summary. To view in full visit <https://peerj.com/about/editorial-criteria/>

## 7 Standout reviewing tips

3



The best reviewers use these techniques

### Tip

### Example

**Support criticisms with evidence from the text or from other sources**

*Smith et al (J of Methodology, 2005, V3, pp 123) have shown that the analysis you use in Lines 241-250 is not the most appropriate for this situation. Please explain why you used this method.*

**Give specific suggestions on how to improve the manuscript**

*Your introduction needs more detail. I suggest that you improve the description at lines 57- 86 to provide more justification for your study (specifically, you should expand upon the knowledge gap being filled).*

**Comment on language and grammar issues**

*The English language should be improved to ensure that your international audience can clearly understand your text. I suggest that you have a native English speaking colleague review your manuscript. Some examples where the language could be improved include lines 23, 77, 121, 128 - the current phrasing makes comprehension difficult.*

**Organize by importance of the issues, and number your points**

1. Your most important issue
2. The next most important item
3. ...
4. The least important points

**Give specific suggestions on how to improve the manuscript**

*Line 56: Note that experimental data on sprawling animals needs to be updated. Line 66: Please consider exchanging "modern" with "cursorial".*

**Please provide constructive criticism, and avoid personal opinions**

*I thank you for providing the raw data, however your supplemental files need more descriptive metadata identifiers to be useful to future readers. Although your results are compelling, the data analysis should be improved in the following ways: AA, BB, CC*

**Comment on strengths (as well as weaknesses) of the manuscript**

*I commend the authors for their extensive data set, compiled over many years of detailed fieldwork. In addition, the manuscript is clearly written in professional, unambiguous language. If there is a weakness, it is in the statistical analysis (as I have noted above) which should be improved upon before Acceptance.*

# Paleohistology of the intercentra of North American metoposaurids from the Upper Triassic of Petrified Forest National Park (Arizona, USA) with implications for the taxonomy and ontogeny of the group

Bryan M Gee <sup>Corresp., 1</sup>, William G Parker <sup>2</sup>, Adam D Marsh <sup>2</sup>

<sup>1</sup> Department of Biology, University of Toronto Mississauga, Ontario, Canada

<sup>2</sup> Division of Science and Resource Management, Petrified Forest National Park, Arizona, United States of America

Corresponding Author: Bryan M Gee

Email address: bryan.gee@mail.utoronto.ca

Metoposaurids are temnospondyl amphibians that are commonly collected from the Chinle Formation deposits of North America. Two species, *Koskinondon perfectus* and *Apachesaurus gregorii* are known from Petrified Forest National Park, AZ, USA. Small, elongate intercentra are the single diagnostic postcranial characteristic of the smaller *A. gregorii*. However, a poor understanding of the earliest life stages of *K. perfectus* and other large metoposaurids makes it unclear whether the proportions of the intercentra are a diagnostic feature for species discrimination or whether they are influenced by ontogeny. Previous work on metoposaurid intercentra has proven that ontogenetic information can be extrapolated from histological analyses. Here we perform a histological analysis of metoposaurid intercentra from Petrified Forest National Park and our results suggest that the elongate intercentra are the consequence of ontogenetic variation rather than speciation.

**Paleohistology of the intercentra of North American metoposaurids from the Upper  
Triassic of Petrified Forest National Park (Arizona, USA) with implications for the  
taxonomy and ontogeny of the group**

Bryan M. Gee<sup>1</sup>; William G. Parker<sup>2</sup>; Adam D. Marsh<sup>2</sup>

<sup>1</sup>Department of Biology, University of Toronto Mississauga, ON, Canada

<sup>2</sup>Division of Science and Resource Management, Petrified Forest National Park, AZ, USA

Corresponding author:

Bryan M. Gee

Corresponding email: [bryan.gee@mail.utoronto.ca](mailto:bryan.gee@mail.utoronto.ca)

**Abstract.** Metoposaurids are temnospondyl amphibians that are commonly collected from the Chinle Formation deposits of North America. Two species, *Koskinondon perfectus* and *Apachesaurus gregorii* are known from Petrified Forest National Park, AZ, USA. Small, elongate intercentra are the single diagnostic postcranial characteristic of the smaller *A. gregorii*. However, a poor understanding of the earliest life stages of *K. perfectus* and other large metoposaurids makes it unclear whether the proportions of the intercentra are a diagnostic feature for species discrimination or whether they are influenced by ontogeny. Previous work on metoposaurid intercentra has proven that ontogenetic information can be extrapolated from histological analyses. Here we perform a histological analysis of metoposaurid intercentra from Petrified Forest National Park and our results suggest that the elongate intercentra are the consequence of ontogenetic variation rather than speciation.

**Introduction.** Metoposaurids are Late Triassic temnospondyl amphibians with a global distribution and are some of the most commonly collected fossils from freshwater depositional settings in the Chinle Formation (Hunt, 1993). There are presently three valid taxa of metoposaurids in North America: two of large size, *Koskinonodon perfectus* and *K. bakeri*, and one of small size, *Apachesaurus gregorii* (Case, 1922, 1931; Branson & Mehl, 1929; Hunt, 1993; Mueller, 2007). Two of these, *K. perfectus* and *A. gregorii* are known from Petrified Forest National Park (PEFO), AZ, USA (Hunt & Lucas, 1993; Long & Murry, 1995; Heckert & Lucas, 2002; Parker & Martz, 2011). The former is common in the lower units within the Chinle Formation (Blue Mesa Member and lower part of the Sonsela Member) and is rare in the upper units (the upper part of the Sonsela Member and the Petrified Forest Member) (Hunt & Lucas, 1993; Heckert & Lucas, 2002; Parker & Martz, 2011). *A. gregorii* demonstrates the opposite pattern of stratigraphic distribution (Parker and Martz, 2011). Although fossils of *A. gregorii* are relatively common, the vast majority of them consist of isolated, elongate intercentra. Additionally, while the diagnosis of *A. gregorii* includes a wide set of cranial traits, only a shallow otic notch can be confirmed by more than one specimen (Spielmann & Lucas, 2012). Finally, while size has frequently been used as an informal characteristic in identifying specimens (*A. gregorii* being significantly smaller than all other metoposaurid taxa), this is not a reliable metric given the role of ontogeny in changing body size (Horner, De Ricqlès & Padian, 1998; Horner & Goodwin, 2009; Werning, 2012). As a result, the diagnosis of *A. gregorii* based

on elongate intercentra is tentative in the absence of multiple specimens that can confirm more of the diagnostic cranial features. Because growth series for North American metoposaurids are not well known, particularly among the earliest life stages, it remains unclear whether the diagnostic anatomy of *A. gregori* is the product of speciation or if it is merely a misinterpretation of features influenced by ontogeny. Such a possibility is rarely considered in determining whether small metoposaurid specimens are skeletally mature individuals of *A. gregorii* or skeletally immature individuals of either *Koski* or *oa* species. In this study, we focus on analyzing the single diagnostic postcranial trait of *A. gregorii*, elongate intercentra.

Bone histology is a common method used to study ontogeny in a variety of extinct taxa, often by comparison to extant members of these clades (Padian, 2013). Although the majority of paleohistological inquiries have centered on amniotes, several workers have previously performed histological analyses on temnospondyls (e.g., Steyer et al., 2004; Witzmann & Soler-Gijon, 2010; Sanchez & Schoch, 2013). Most of these analyses have examined long bones, as is conventional for other tetrapods (e.g. Konietzko-Meier & Sander, 2013). Histology of temnospondyl intercentra has been performed only a handful of times (e.g., Mukherjee, Ray & Sengupta, 2010; Konietzko-Meier, Danto & Gadek, 2014; Danto, Witzmann & Fröbisch, 2016), and the only previous examination of metoposaurid intercentra was conducted on the European taxon *Metoposaurus krasiejowensis* (Konietzko-Meier, Bodzioch & Sander, 2012). Metoposaurid intercentra spanning a wide size range are commonly recovered elements at PEFO, making them more accessible for histology than the relatively rare limb elements. This study seeks to provide an alternative approach to comparisons of external morphology in order to evaluate the potential for metoposaurid intercentra proportions to be influenced by ontogeny rather than speciation.

**Keywords:** paleohistology, ontogeny, metoposaurid

**Institutional Abbreviations:** NMMNH: New Mexico Museum of Natural History and Science, Albuquerque, NM, USA; PEFO: Petrified Forest National Park, AZ, USA; UOPB, University of Opole, Department of Biosystematics, Opole, Poland.

## Materials and Methods.

# 94 *Selection of specimens*


95 All material referenced here was collected from the Late Triassic sedimentary rocks of the  
 96 Chinle Formation at Petrified Forest National Park, AZ, USA. Metoposaurids are found  
 97 throughout three commonly occurring units of the Chinle (the Blue Mesa Member, Sonsela  
 98 Member, and Petrified Forest Member), but there are disparate relative abundances of large and  
 99 small metoposaurids throughout the stratigraphic column. Eight of the ten elements were  
 100 selected with the goal of sampling an intercentrum of shortened proportions normally referred to  
 101 *K. perfectus* and an intercentrum of elongate proportions normally referred to *A. gregorii* from  
 102 the same stratigraphic horizon, if not the same locality (Table 1, Fig. 3). PEFO 4826 and PEFO  
 103 38726 are from locality PFV 122 in the Blue Mesa Member (Fig. 1-2). PEFO 38645 is from PFV  
 104 040 in the Petrified Forest Member (Fig. 1-2). PEFO 36874 and PEFO 16696 (two and three  
 105 intercentra, respectively) are from a locality (PFV 215) in the Petrified Forest Member (Fig. 1-2).  
 106 Elements are assigned to the same specimen number on the basis of physical proximity during  
 107 collection and general taxonomic identity and should not be interpreted to mean that the elements  
 108 are from the same individual. The final two intercentra, belonging to PEFO 35392 (also from  
 109 PFV 215), were selected because of their association with a skull of a small metoposaurid that  
 110 was interpreted to be a juvenile *K. perfectus* (B.M. Gee & W.G. Parker, unpublished data).  
 111 Specimens were measured using the same standards as Konietzko-Meier, Bodzioch & Sander  
 112 (2012). The overall size range of the elements sampled in this study (mediolateral width between  
 113 9.81 mm and 55.32 mm) is similar to that sampled by the motivational study (mediolateral width  
 114 between 20.1 mm and 71 mm; Konietzko-Meier, Bodzioch & Sander, 2012).

# 116 *Classification of specimens' axial position*

117 Because North American metoposaurids, especially those from PEFO, are rarely articulated,  
 118 determining the exact serial position of the studied vertebrae remains difficult. Vertebrae are  
 119 placed using previously-outlined criteria (Sulej, 2007), but it should be noted that these criteria  
 120 were used in the description of *Metoposaurus krasiejowensis* and it remains unknown what  
 121 differences may exist in the vertebral column between the European and North American taxa,  
 122 especially in the absence of preserved neural or haemal arches. Additionally, intraspecific  
 123 variation in North American metoposaurids is poorly known; thus the serial position of smaller  
 124 intercentra is the most tentative.



125

126 *Thin section preparation and imaging* 

127 The intercentra were first cleaned using a toothbrush and water to remove excess matrix before  
 128 being consolidated with Paraloid B-72 (Rohm and Haas) dissolved in acetone. All specimens  
 129 were molded and casted according to PEFO museum standards, with Carbowax (molecular  
 130 weight 4000; Dow) added to stabilize cracks and other fragile areas. After creating two-part  
 131 molds using (I need to send you latex info), the Carbowax was removed using a brush and warm  
 132 water. All specimens were impregnated in a polyester resin mixture of Castolite™ AC and  
 133 hardener (Eager Polymers) at a ratio of 1 oz of Castolite™ to 12 drops of hardener. The  
 134 specimens were placed in a vacuum chamber to evacuate gas from the resin and then allowed to  
 135 cure for a minimum of 24 hours. Because the primary focus of the study was to assess the  
 136 ontogenetic stage of various intercentra to determine whether small, elongate intercentra ascribed  
 137 to *A. gregorii* belonged to juveniles of *K. perfectus*, we decided to focus on sagittal cuts (down  
 138 the midline in the anteroposterior axis) based on the amount of ontogenetic information that  
 139 could be derived from the different planes in the analysis of Konietzko-Meier, Bodzioch &  
 140 Sander (2012). All specimens were cut using an automated IsoMet 1000 Precision Saw  
 141 (Buehler). The cut surface of the desired block and its respective thin section were prepared by  
 142 polishing each with a 600-mesh silicon carbide on (include make, model, rpm with parent  
 143 company in parentheses). Both surfaces were rinsed with ethanol and then attached to plexiglass  
 144 slides using Scotch-Weld Instant Adhesive (CA40; 3M). The sections were allowed to dry for a  
 145 minimum of 1 hour. All specimens except PEFO 38726 were cut to a height of 0.7 mm using the  
 146 IsoMet 1000 Precision Saw. PEFO 38726 was too large to be cut by the automatic saw, so it was  
 147 cut manually by hand with a larger saw fitting for the IsoMet. All specimens were polished in the  
 148 following sequence: Hillquist 1010 grinding cup, 600-mesh grit, 1000-mesh grit, 1-micron grit.  
 149 PEFO 38726 was polished on a 600-mesh lap wheel before polishing on the Hillquist to remove  
 150 uneven surfaces from the manual cut. The thin sections were gradually ground down with  
 151 repeated examination under a compound microscope to evaluate their optical clarity. All  
 152 polishing after the Hillquist step was done manually on glass plates. Thin sections were imaged  
 153 on a Nikon Instruments AZ100 Multizoom microscope fitted with AZ-Plan Apo 0.5x and AZ-  
 154 Fluor 5x objective lenses, an AZ-RP rotatable polarizer plate, and a DS-Fi2 digital camera  
 155 mount. NIS-Elements imaging software was used for this study.

# Results.

## Microanatomy and general histology

Overall, the composition and structure of the intercentra sampled is very similar to those that were described for *Metoposaurus krasiejowensis* (Konietzko-Meier, Bodzioch & Sander, 2012). At peripheral surfaces that were preserved, endochondral bone is found on the anterior and posterior faces and at the dorsal surface where the intercentrum would have been attached to the neural spine (Fig. 4). The ventral surface is formed by endochondral trabecular bone in younger individuals and by an external cortex in more mature individuals (Fig. 4). With the exception of the smallest intercentra that fall outside of the lower size bound of the sampled specimens of *M. krasiejowensis* (Konietzko-Meier, Bodzioch & Sander, 2012), a distinct region of periosteal bone is present in a triangular shape, with the apex ventral to the geometrical center of the element in all but some of the largest intercentra (Fig. 4G-H). This triangular region is separated from the endochondral region by obliquely-oriented trabeculae (Fig. 4). Within the periosteal region, the layers are densely packed and oriented parallel to the ventral surface of the intercentrum in contrast to the random arrangement of endochondral bone (Fig. 4). In some of the larger specimens, the periosteal region lacks the densely packed matrix (Fig. 4B, 4H-I). This does not appear to be ontogenetic in nature because PEFO 38726, the largest specimen, features a densely layered periosteal region in the absence of secondary mineral precipitation that characterizes all specimens with open periosteal regions (Fig. 4J). Additionally, some of the smaller specimens, such as PEFO 36874a, feature reduced secondary mineralization that only damages the local areas of the periosteal region in which it occurs (Fig. 4B).

For this study, we utilize the formal Histological Ontogenetic Stages (HOS) that were created for *M. krasiejowensis* by Konietzko-Meier, Bodzioch, & Sander (2012). The nature of the periosteal bone is used to characterize the ontogenetic stage of an individual; HOS 1 lacks any periosteal ossification, HOS 2 features a wide periosteal bone, HOS 3 features decreased vascularization in the external cortex, and HOS 4 features LAGs in the external cortex (Konietzko-Meier, Bodzioch, & Sander 2012). The ontogenetic assignments are summarized below in Table 2.

*PEFO 16696* (Fig. 4B, 4D, 4H, 5C, 6C, 7C, 8C-D): *PEFO 16696a* is similar to *PEFO 4826* in having a fully open notochordal channel filled with secondary minerals (Fig. 5C). The periosteal region is semi-circular as in the smaller intercentra, but the layered matrix is significantly more disperse (Fig. 6C). The presence of secondary mineral precipitates, a feature also seen in the periosteal region of *PEFO 35392*, *PEFO 36874b*, *PEFO 38645*, and *PEFO 16696c*, appears to be responsible for the absence of densely layered matrix in the region (Fig 6C). Additionally, the endochondral bone in the dorsal half of *PEFO 16696a* is significantly more disperse than in larger specimens sampled here, although the endochondral bone on the articular faces is thicker and more densely packed, as observed in all other intercentra (Fig. 4B, Fig. 7C). Relative to larger intercentra, the marginal endochondral bone appears to be more vascularized. *PEFO 16696b* and *PEFO 16696c* share many features with other large intercentra. The periosteal region is triangular in shape and consists of a parallel-layered matrix (Fig. 8D). In *PEFO 16696b*, the apex that terminates ventral to the mid-height of the element, while in *PEFO 16696c*, it terminates at or slightly above this point (Fig. 4D, Fig. 4H). In *PEFO 16696c*, some layers of the periosteal region appear to have been destroyed by precipitation of secondary minerals, a recurring feature in some of the larger intercentra, which makes it difficult to identify the exact point of termination of the apex. The endochondral bone is thickest at the articular surfaces and is more disperse in the internal cavity. There is no evidence of an external cortex in *PEFO 16696a* and *PEFO 16696b*. In *PEFO 16696c*, an external cortex is present, but it is well vascularized and shows no evidence of LAGs (Fig. 8C). We assign *PEFO 16696a* and *PEFO 16696b* to HOS 2. *PEFO 16696c* is assigned to HOS 3 but is considered to be relatively immature in comparison to other specimens of the same assignment.

*PEFO 35392* (Fig. 4G, 4I, 8B): Both of these elements are associated with a partial skull that was interpreted as a juvenile *K. perfectus* by B.M. Gee & W.G. Parker (unpublished data). The histological characterization of these intercentra supports this interpretation, as they feature a relatively wide periosteal region and a moderate degree of vascularization in the external cortical region (Fig. 4G, 4I). Both elements are similar to each other and to other intercentra lacking a notochordal channel that were sampled in this study. The periosteal region is triangular in shape with an apex that terminates well below the mid-height of the intercentrum in *PEFO 35392a* (Fig. 4G) and an apex that terminates around that point in *PEFO 35392b* (Fig. 4I). The matrix of

parallel layers is much less dense and coincides with the presence of secondary carbonate minerals, which likely damaged the region, making it difficult to discern the exact point at which the apex terminates in PEFO 35392b (Fig. 4I). The endochondral bone is relatively intact and is similar to other intercentra in being densest at the articular faces and randomly distributed throughout the internal cavity. A weathered external cortex is preserved in both of the specimens, but appears to still be relatively well vascularized and shows no evidence of LAGs where present (Fig. 8B). We assign both specimens to HOS 3.

*PEFO 36874* (Fig. 4A, 4F, 5B, 6B, 7B): The smaller of the two elements assigned to this specimen (*PEFO 36874a*) differs from *PEFO 4826* and *PEFO 16696a* in having a notochordal channel that appears to be in the early stages of ossification. Tissue deposition originates around the geometric center of the element and probably spread outward throughout ossification based on the characterization of the notochordal pits in larger specimens (Fig. 5B). In this specimen, tissue from the two halves appears to have recently connected prior to the death of the individual. The overall shape of the periosteal region of *PEFO 36874a* is similar to the semi-circular contour of the other small intercentra (Fig. 6B). *PEFO 36874b* features a typical morphology of the larger intercentra sampled in this study: a triangular periosteal region with an apex terminating ventral to the mid-height of the element, dense endochondral bone on the articular surfaces, and more disperse, vascularized endochondral bone in the internal cavity (Fig. 4). As in several other intercentra, the periosteal region lacks a densely layered matrix but co-occurs with a similar concentration of secondary carbonate minerals. An external cortex does not appear to be present in *PEFO 36874a*, and in *PEFO 36874b*, it is highly vascularized with no evidence of LAGs (Fig. 4). We assign *PEFO 36874a* to HOS 2 and *PEFO 36874b* to HOS 3.

*PEFO 38645* (Fig. 4E, 8A): This specimen shows no evidence of a notochordal channel. The periosteal region is comparable to other specimens in having a parallel-layered matrix and an apex that terminates below the mid-height of the intercentrum (Fig. 4E). The periosteal region lacks a densely layered matrix, as in *PEFO 35392* and *PEFO 36874b*, but also features a high degree of secondary carbonate precipitation that likely damaged the internal structure (Fig. 4E). One articular surface was damaged during preparation of the thin section, but the other shows a dense endochondral bone layer with tighter packing than the elements of *PEFO 35392*. Similar to

PEFO 36874, a posterior protrusion on the dorsal surface that may be a remnant of the neural arch is preserved (Fig. 4E). The remainder of the endochondral bone in the internal cavity is otherwise modestly vascularized and randomly oriented. The external cortex is relatively well preserved and compact, similar to PEFO 38726, but there is no evidence of LAGs or any taphonomic damage that may have erased them (Fig. 8A). We assign this specimen to HOS 3 and note that it is more mature than the elements of PEFO 35392.

*PEFO 38726* (Fig. 4J, 8D): This specimen is the largest analyzed in this study and shows no evidence of a notochordal channel. The periosteal region consists of a dense matrix of parallel layers and is triangular in shape with an apex that terminates at or before the mid-height of the element (Fig. 4J). The external cortex of this specimen is relatively well preserved and shows a reduced degree of vascularization compared to the smaller specimens. At least two light-colored bands can be seen in the cortex and run parallel to the ventral surface of the intercentrum (Fig. 8D). They are continuous throughout the well-preserved portion of this area, which leads us to tentatively conclude that these are LAGs. As in other intercentra, the endochondral bone on the articular surfaces is thicker and more densely packed than in the internal cavity. On the dorsal surface, an elevated posterior protrusion may be the remnants of a neural arch that was lost during preservation (Fig. 4J). We assign this specimen to HOS 4.

*PEFO 4826* (Fig. 4C, 5A, 6A, 7A): This specimen is the largest of the three intercentra that feature an open notochordal channel. The notochordal channel is obstructed only by secondary matrix; its dorsal and ventral walls are nearly flat (Fig. 5A). The periosteal region is semi-circular, as in the PEFO 16696a and PEFO 36874a, with a dense matrix of parallel layers running in the anterior-posterior axis (Fig. 6A). There is no evidence of taphonomic damage that resulted in the absence of a compact external cortex with LAGs. The endochondral bone in the dorsal portion of the intercentrum shows an intermediate degree of vascularization in being more densely packed than the other two small intercentra and less densely packed than in larger intercentra with a closed notochordal channel (Fig. 7A). Dense endochondral bone also forms the margins on the anterior and posterior articular surfaces. The dorsal margin of the element is slightly damaged, which is common in North American metoposaurids owing to the removal of the neural arches during preservation. We assign this specimen to HOS 2.

280

281 **Discussion.** The most significant finding of this study is the confirmation that, at least in some  
 282 instances, small intercentra of proportions referable to *A. gregorii* belong to highly immature  
 283 individuals. Two prominent features inform the ontogenetic assignment of these specimens: (1) a  
 284 perforate notochordal channel and (2) a wide, more semi-circular periosteal region (Fig. 5-6).  
 285 These structures are found in the three smallest intercentra (PEFO 4826, PEFO 16696a, PEFO  
 286 36874a) and provide insight into the ontogenetic changes in the internal structure of the axial  
 287 column in metoposaurids. We are confident that the open notochordal channel is a juvenile  
 288 feature because its closure is widespread in Triassic temnospondyls, including metoposaurids  
 289 (Warren & Snell, 1991). The notochordal channel closes and is gradually reduced to a pair of  
 290 perforations, one on each articular surface, that migrate dorsally and eventually disappear in  
 291 some species (Warren & Snell, 1991; Danto, Witzmann & Fröbisch, 2016). Based on  
 292 comparisons to described vertebral series in *M. krasiejowensis*, *M. bakeri*, *Dutuitosaurus*  
 293 *ouazzoui* and isolated intercentra of *K. perfectus*, this pattern often terminates in an entirely  
 294 smooth articular surface with no notochordal perforation in mature individuals (Case, 1932;  
 295 Dutuit, 1976; Warren & Snell, 1991; Sulej, 2007). Additionally, we can be certain that the  
 296 notochordal channel does close in smaller individuals with elongate intercentra based on PEFO  
 297 36874a, which captures the onset of this ossification and is discussed further below (Fig. 5B).  
 298 The designation of the three smallest intercentra as belonging to juvenile individuals is also  
 299 supported by the wide periosteal region, which originates near the anteroventral and  
 300 posteroventral margins, forming a shallow concave depression rather than the distinct triangle  
 301 seen in larger intercentra of this study and the intercentra of *Metoposaurus* (Konietzko-Meier,  
 302 Bodzioch & Sander, 2012). In all three of the smallest PEFO specimens, the apex of the  
 303 periosteal region terminates well before reaching the dorsal surface of the ventral half (Fig. 6).  
 304 Finally, the small intercentra show other evidence of a relatively immature ontogenetic stage,  
 305 such as the absence of thick ventral trabeculae near the external surface, the absence of LAGs,  
 306 and less densely packed endochondral bone in the dorsal portion of the intercentrum in  
 307 comparison to larger specimens (Fig. 4A-C, Fig. 5-6). As a result, we can be confident that the  
 308 ossification of the notochordal channel did not occur relatively late in ontogeny and conclude  
 309 that all three of the small intercentra belong to an early ontogenetic stage of a large metoposaurid  
 310 rather than to *A. gregorii*. Larger sampled intercentra also show evidence of relative immaturity

up to the largest specimen, PEFO 38726, when LAGs appear in the external cortex (Fig. 8D). Although the material is from a variety of localities and stratigraphic horizons, increased size of the sampled intercentra always produced more ontogenetically mature structures, leading us to conclude that the sampled material can be compiled into a composite growth series. Because *K. bakeri* has not been identified west of Texas, and its intercentra differ from that of *K. perfectus* with regard to the notochordal channel (discussed below), we tentatively assign this material to *K. perfectus*, with the understanding that future revision may be necessary as more diagnostic material is recovered (Hunt, 1993; Long & Murry, 1995). It is possible that the onset of ossification of the notochordal channel reflects a milestone in the development of *K. perfectus*. In light of the hypothesis suggesting that *Koskinonodon* could have had ecologically separated life stages (Rinehart et al., 2009), the ossification of the intercentra could potentially represent the onset of a more aquatic lifestyle.

This study has also produced an unexpected finding that suggests some differences in the ontogenetic trajectory of *K. perfectus* in relation to other metoposaurids with known vertebral columns. In the original description of *K. bakeri*, Case (1932) noted that the presence of a notochordal channel and its persistence as reduced perforations on the articular surfaces in more mature specimens differed from other metoposaurid specimens from Texas, presumably of *K. perfectus*, in that the known material of the latter lacked any sort of perforation. This pattern also appears in the intercentra of *K. perfectus* that are described or figured in other publications (e.g., Colbert & Imbrie, 1956; Hunt, 1993; Long & Murry, 1995; Spielmann & Lucas, 2012). We have also found this same pattern in an informal survey of several dozen metoposaurid intercentra in the collections at PEFO. This suggests that with regards to timing, the ossification of the notochordal canal occurs much earlier in *K. perfectus*. We also note that the smallest specimen analyzed by Konietzko-Meier, Bodzioch & Sander (2012), an early juvenile (UOPB 00117), is larger than two of the three small intercentra sampled here (PEFO 16696a, PEFO 36874a) but is classified as being more ontogenetically immature (HOS 1) than either due to the absence of periosteal ossification (Fig. 5, Table 2). It may be that *K. perfectus* juveniles experienced a relatively rapid burst of growth and tissue reorganization within the skeleton in comparison to *M. krasiejowensis*, possibly as a result of environmental triggers, but this hypothesis requires additional sampling to test. Finally, only the largest intercentra sampled in our study (PEFO




38726) contains possible LAGs in the external cortex (Fig. 8D). This element is most comparable in size to UOPB 00115, which they classified as a late juvenile (Konietzko-Meier, Bodzioch & Sander, 2012) and in which no LAGs were observed. This suggests that *K. perfectus* may have reached maturity slightly later than *M. krasiejowensis*, but again, additional sampling is required. Variability in ontogenetic trajectories has been previously documented between *D. ouazzoui* and *M. krasiejowensis* as a result of differing environmental conditions (Konietzko-Meier & Klein, 2013). As the Chinle depositional basin was positioned closer to the equator in comparison to the environments in which *D. ouazzoui* and *M. krasiejowensis* are found (Steiner & Lucas, 2000; Rowe et al., 2007; Zeigler & Geissman, 2011; Nordt, Atchley & Dworkin, 2015), it is plausible that the paleoenvironment differed sufficiently from both taxa so as to result in a distinct ontogenetic trajectory in *K. perfectus*. Additional sampling of material, particularly limb elements, is needed for comparative analyses to assess this possibility.

The other unexpected finding of this study was an intercentrum (PEFO 36874a) in the process of undergoing ossification of the notochordal channel (Fig. 4B). This was not evident when examining the external morphology of the specimen, as the notochordal channel or pit is usually filled with secondary minerals. Bone tissue can be clearly seen growing into the channel at the geometric center via deposition of bone on the internal sides of the dorsal and ventral halves (Fig. 4B). The dorsal half appears to be contributing more material through bone deposition, but this requires additional specimens to verify (Fig. 4B). Although this specimen is smaller than the more immature PEFO 4826, this does not contradict our ontogenetic assignment based on examination of the external morphology of other small, elongate intercentra at PEFO. There appears to be some variability in the exact timing of the closure of the notochordal channel, as specimens of similar size and proportion exhibit the full range of conditions, from an open channel to a smooth articular surface lacking any trace of the channel. This could be owing to a number of processes that require additional samples to evaluate, such as the progression of ossification of the vertebral column in the anterior-posterior direction or intraspecific variation in the onset of ossification. If the early stages of vertebral ossification were in some way influenced by environmental factors rather than the size of the animal, developmental plasticity, which occurs in both extant and extinct amphibians, could explain how relatively larger intercentra could sometimes be histologically more immature than smaller ones (Newman, 1992; Schoch,



2014). As previously noted, this may also indicate a relatively fast ossification of the notochordal channel.

These findings also provide support of niche partitioning between life stages of metoposaurids  which has been suggested in *Koskinonodon* (Rinehart et al., 2009) and in *Metoposaurus* (Sulej, 2007). Such partitioning could reasonably have created an associated taphonomic bias, which is well documented in both dense bonebeds and more dispersed localities. All known metoposaurid bonebeds have so far produced only large, relatively mature individuals with no evidence of the earliest ontogenetic stages (Case, 1932; Colbert & Imbrie, 1956; Dutuit, 1976; Hunt, 1993; Sulej, 2007; Lucas et al., 2010; Brusatte et al., 2015). Furthermore, although fossils from mature individuals of *K. perfectus* are common in the middle Norian, material referable to juveniles of the taxon is extremely rare, providing another line of support for niche partitioning; to date, only two partial skulls have been described (Zanno et al., 2002; B.M. Gee & W.G. Parker, unpublished data), with a third figured but not described by Hunt (1993). Material of *A. gregorii* is common in the Redonda Formation in New Mexico but occurs mostly within a single quarry (Gregory's quarry, NMMNH locality 485) (Spielmann and Lucas, 2012). As a result, the relative abundance of *A. gregorii* may not be the result of ecological turnover as postulated by Hunt (1993) but may represent the preservation of depositional environments inhabited by juveniles of *K. perfectus*. As bonebeds of mature metoposaurids have been interpreted as evidence of ecological aggregation prior to death, it is not implausible to infer that juveniles may also have naturally aggregated, creating a preservation potential for dense assemblages (Lucas et al., 2010; Brusatte et al., 2015). Based on the isolated and disarticulated nature of most *Apachesaurus* material, we do not believe these deposits represent mass mortality events, but that they are more likely representative of depositional environments frequented by small metoposaurids over longer durations of time. This hypothesis is supported by a previous study that surveyed blue paleosol localities at PEFO and found that material of many rare taxa, as well as that of *A. gregorii*, are found mostly within these uncommon horizons (Loughney, Fastovsky & Parker, 2011). PFV 040, PFV 215, and potentially PFV 122, the three localities from which specimens for this study were sourced, are all blue paleosol horizons. This lithology is interpreted to have formed in low-energy systems, primarily abandoned channels and ponds adjacent to the main river channel, in contrast to the dominant red floodplain deposits in which fossil material is more

fragmentary and isolated (Loughney, Fastovsky & Parker, 2011). The association of *Apachesaurus* material within these blue paleosol localities supports the hypothesis that deposits that are disproportionately skewed toward fossils of small metoposaurids (exemplified by PFV 040 and PFV 215) form in different geologic settings than deposits that are skewed toward large metoposaurids. This in turn supports the hypothesis of natural ecological separation between life stages of metoposaurids. Additionally, taxa that are primarily associated with blue paleosol horizons may not be as stratigraphically restricted as previously thought, and a perceived faunal turnover may in fact be more closely linked to changes in the relative taphonomic conditions of different depositional settings. It is also worth noting that neither *A. gregorii* nor any other diminutive species of metoposaurid is known outside of North America (Long and Murry, 1995; Spielmann & Lucas, 2012). This is at odds with the conjecture by previous authors that *A. gregorii* is the most terrestrial of metoposaurids based on the intercentra and rare appendicular material (Hunt, 1993; Sulej, 2007; Spielmann & Lucas, 2012). If this were true, it would be reasonable to expect the taxon or other similarly adapted forms to disperse more widely than aquatic relatives, especially if the pronounced aridification of the Late Triassic led to significantly reduced aquatic environments (Parker & Martz, 2011; Atchley et al., 2013; Nordt, Atchley & Dworkin, 2015), but this pattern is not seen.

**Conclusions.** These findings reiterate the importance of evaluating the potential for morphological variation to be the result of ontogeny, especially when comparing two taxa of vastly different sizes, such as *A. gregorii* and *K. perfectus*. Although fossils of *A. gregorii* are common in late Norian deposits, the vast majority of this material has consisted of elongate intercentra, which we demonstrate here cannot be considered apomorphic. Limited fragmentary pectoral and pelvic material of *A. gregorii* has been described in the literature, but no justification for ascribing it to the taxon has ever been provided (Hunt, 1993; Long & Murry, 1995; Spielmann & Lucas, 2012). Although this material was recovered from the same quarry as cranial and vertebral material, there is no published work suggesting that any of it was found in articulation with any of the diagnostic cranial material (Spielmann & Lucas, 2012). North American metoposaurid specimens are frequently isolated or disarticulated, but this does not negate the importance of reevaluating the taxonomic identity of this material to determine whether they preserve robust diagnostic traits. It is possible that these assignments were made

solely on the basis of diminutive size (Hunt, 1993; Long & Murry, 1995; Spielmann & Lucas, 2012), which cannot be utilized as in species discrimination given the role of ontogeny in producing morphological variation associated with different size bins (Steyer, 2000; Horner and Goodwin, 2009; Witzmann, Scholz & Ruta, 2009). Similarly, although a large number of diagnostic cranial characters have been identified for *A. gregorii*, only a single character, the shallow otic notch, can be confirmed in any specimens beyond the holotype (Spielmann & Lucas, 2012). The potential for these cranial landmarks to be ontogenetically influenced has not been sufficiently addressed by past workers, in spite of the widespread documentation of morphological changes associated with ontogeny in both extant and extinct amphibians (Hanken, 1992; Fröbisch et al., 2010; Schoch, 2014). For example, studies of other Triassic temnospondyls have shown that the otic notch, occipital condyles, and cultriform process (by virtue of its relationship with the interpterygoid vacuities) all play a role in bite force mechanics (Fortuny, Marcé-Nogué & Galobart, 2012; Fortuny et al., 2016; Lautenschlager, Witzmann & Werneburg, 2016). Based on these findings, the presence of shallow otic notches, reduced projection of the occipital condyles, and a wider cultriform process (all supposedly diagnostic traits of *A. gregorii*) may in fact be influenced by changing biomechanical demands throughout ontogeny, rather than being the result of speciation. The potential for intraspecific variation to exert an influence on metoposaurid morphology has also not been well studied in North American taxa even though studies of bonebeds of *M. krasiejowensis* and *M. algarvensis* have demonstrated a higher degree of variability in many cranial regions than previously thought (Sulej, 2007; Brusatte et al., 2015).

Finally, we believe that our results provide one line of evidence that *A. gregorii* is not in fact a distinct species, but rather that it is an early ontogenetic stage of *K. perfectus*. The stratigraphic distribution that is alleged to reflect ecological turnover is actually controlled by taphonomic bias that results from niche partitioning between different life stages of *K. perfectus*. The role of ontogeny and intraspecific variation in producing morphological variation in features such as cranial suture patterns, the basicranium, and the otic notch remain relatively unexplored in North American metoposaurids. Discovery and study of additional juvenile specimens is needed to establish a more robust ontogenetic characterization of the earliest stages of metoposaurid development, but our study has also demonstrated that underutilized methods of analysis such as

paleohistology on existing specimens can shed new light on the paleobiology of extinct taxa with implications for taxonomy and ontogeny.

**Acknowledgements.** Thanks to Matt Smith (PEFO museum curator) for providing access to specimens for histological analysis and to Brad Traver (PEFO Superintendent) for granting permission to conduct the destructive analyses. Thanks to Cathy Lash (PEFO fossil preparator) for assistance with molding and casting of the specimens and to Yara Haridy (University of Toronto) for instruction and guidance on preparation and imaging of thin sections. This is Petrified Forest National Park Paleontological Contribution no. 49.

## References



- Atchley, S.C., Nordt, L.C., Dworkin, S.I., Ramezani, J., Parker, W.G., Ash, S.R., and Bowring, S.A. 2013. A linkage among Pangean tectonism, cyclic alluviation, climate change and biologic turnover in the Late Triassic: the record from the Chinle Formation, southwestern United States. *Journal of Sedimentary Research* 83(12): 1146-1161. DOI: 10.2110/jsr.2013.89
- Branson, E.B. and Mehl, M.G. 1929. Triassic amphibians from the Rocky Mountain region. *University of Missouri Studies* 4: 155-239.
- Brusatte, S.L., Butler, R.J., Mateus, O. and Steyer, J.S. 2015. A new species of *Metoposaurus* from the Late Triassic of Portugal and comments on the systematics and biogeography of metoposaurid temnospondyls. *Journal of Vertebrate Paleontology* 35(3), e912988. DOI: 10.1080/02724634.2014.912988
- Case, E.C. 1922. New reptiles and stegocephalians from the Upper Triassic of western Texas. *Carnegie Institution of Washington* 321: 7-84.
- Case, E.C. 1931. Description of a new species of *Buettneria*, with a discussion of the brain case. *Contributions from the Museum of Paleontology, University of Michigan* 3(11): 187-206.
- Case, E.C. 1932. A collection of stegocephalians from Scurry County, Texas. *Contributions from the Museum of Paleontology, University of Michigan* 4: 1-56.
- Colbert, E.H., and Imbrie, J. 1956. Triassic metoposaurid amphibians. *Bulletin of the American Museum of Natural History* 110(6): 399-452.

- Danto, M., Witzmann, F. and Fröbisch, N.B. 2016. Vertebral Development in Paleozoic and Mesozoic Tetrapods Revealed by Paleohistological Data. PLoS ONE 11(4): e0152586. DOI: 10.1371/journal.pone.0152586
- Dutuit, J.M. 1976. Introduction à l'étude paléontologique du Trias continental marocain. Description des premiers stegocephales recueillis dans le couloir d'Argana (Atlas occidental). Memoires du Museum National d'Histoire Naturelle, Paris, Series C 36: 1–253.
- Fortuny, J., Marcé-Nogué, J., Steyer, J.S., de Esteban-Trivigno, S., Mujal, E. and Gil, L. 2016. Comparative 3D analyses and palaeoecology of giant early amphibians (Temnospondyli: Stereospondyli). Scientific Reports 6: 30387. DOI: 10.1038/srep30387
- Fortuny, J., Marcé-Nogué, J., Gil, L. and Galobart, À. 2012. Skull mechanics and the evolutionary patterns of the otic notch closure in capitosaur (Amphibia: Temnospondyli). The Anatomical Record 295(7): 1134-1146. DOI: 10.1002/ar.22486
- Fröbisch, N.B., Olori, J.C., Schoch, R.R. and Witzmann, F. 2010. Amphibian development in the fossil record. Seminars in Cell & Developmental Biology 21(4): 424-431. DOI: 10.1016/j.semcdb.2009.11.001
- Hanken, J. 1992. Life history and morphological evolution. Journal of Evolutionary Biology 5(4): 549-557.
- Heckert, A.B., and Lucas, S.G. 2002. Revised Upper Triassic stratigraphy of the Petrified Forest National Park, Arizona, U.S.A.; pp. 1-36 in A.B. Heckert and S.G. Lucas (eds.), Upper Triassic Stratigraphy and Paleontology. New Mexico Museum of Natural History and Science Bulletin 21. New Mexico Museum of Natural History and Science, Albuquerque.
- Horner, J.R. and Goodwin, M.B. 2009. Extreme cranial ontogeny in the Upper Cretaceous dinosaur *Pachycephalosaurus*. PLoS ONE 4(10): e7626. DOI: 10.1371/journal.pone.0007626
- Horner, J.R., De Ricqlès, A., and Padian, K. 1998. Long bone histology of the hadrosaurid dinosaur *Maiasaura peeblesorum*: growth dynamics and physiology based on an ontogenetic series of skeletal elements. Journal of Vertebrate Paleontology 20(1): 115-129.

- Hunt, A.P. 1993. A revision of the Metoposauridae (Amphibia: Temnospondyli) and description of a new genus from western North America; pp. 67-97 in M. Morales (ed.), Aspects of Mesozoic Geology and Paleontology of the Colorado Plateau. Museum of Northern Arizona Bulletin 59. Museum of Northern Arizona, Flagstaff.
- Hunt, A.P., and Lucas, S.G. 1993. Taxonomy and stratigraphic distribution of Late Triassic metoposaurid amphibians from Petrified Forest National Park, Arizona. Journal of the Arizona-Nevada Academy of Science 27(1): 89-96.
- Konietzko-Meier, D. and Klein, N. 2013. Unique growth pattern of *Metoposaurus diagnosticus krasiejowensis* (Amphibia, Temnospondyli) from the Upper Triassic of Krasiejów, Poland. Palaeogeography, Palaeoclimatology, Palaeoecology 370: 145-157. DOI: 10.1016/j.palaeo.2012.12.003
- Konietzko-Meier, D. and Sander, P.M. 2013. Long bone histology of *Metoposaurus diagnosticus* (Temnospondyli) from the Late Triassic of Krasiejów (Poland) and its paleobiological implications. Journal of Vertebrate Paleontology 33(5):1003-1018. DOI: 10.1080/02724634.2013.765886
- Konietzko-Meier, D., Bodzioch, A. and Sander, P.M. 2012. Histological characteristics of the vertebral intercentra of *Metoposaurus diagnosticus* (Temnospondyli) from the Upper Triassic of Krasiejów (Upper Silesia, Poland). Earth and Environmental Science Transactions of the Royal Society of Edinburgh 103(3-4): 237-250. DOI: 10.1017/S1755691013000273
- Konietzko-Meier, D., Danto, M. and Gądek, K. 2014. The microstructural variability of the intercentra among temnospondyl amphibians. Biological Journal of the Linnean Society 112(4): 747-764.
- Lautenschlager, S., Witzmann, F. and Werneburg, I. 2016. Palate anatomy and morphofunctional aspects of interpterygoid vacuities in temnospondyl cranial evolution. The Science of Nature 103(9-10): 79. DOI: 10.1007/s00114-016-1402-z
- Long, R.A. and Murry, P.A. 1995. Late Triassic (Carnian and Norian) Tetrapods from the Southwestern United States. New Mexico Museum of Natural History and Science Bulletin 4. New Mexico Museum of Natural History and Science, Albuquerque.
- Loughney, K.M., Fastovsky, D.E. and Parker, W.G. 2011. Vertebrate fossil preservation in blue paleosols from the Petrified Forest National Park, Arizona, with implications for

- vertebrate biostratigraphy in the Chinle Formation. *Palaios*, 26(11): 700-719. DOI: 10.2110/palo.2011.p11-017r
- Lucas, S.G., Rinehart, L.F., Krainer, K., Spielmann, J.A. and Heckert, A.B. 2010. Taphonomy of the Lamy amphibian quarry: a Late Triassic bonebed in New Mexico, USA. *Palaeogeography, Palaeoclimatology, Palaeoecology* 298(3): 388-398. DOI: 10.1016/j.palaeo.2010.10.025
- Mueller, B.D. 2007. *Koskinonodon* Branson and Mehl, 1929, a replacement name for the preoccupied temnospondyl *Buettneria* Case, 1922. *Journal of Vertebrate Paleontology* 27(1): 225-225. DOI: 10.1671/0272-4634(2007)27[225:KBAMAR]2.0.CO;2
- Mukherjee, D., Ray, S. and Sengupta, D.P. 2010. Preliminary observations on the bone microstructure, growth patterns, and life habits of some Triassic temnospondyls from India. *Journal of Vertebrate Paleontology* 30(1): 78-93. DOI: 10.1080/02724630903409121
- Newman, R.A. 1992. Adaptive plasticity in amphibian metamorphosis. *BioScience* 42(9): 671-678.
- Nordt, L., Atchley, S. and Dworkin, S. 2015. Collapse of the Late Triassic megamonsoon in western equatorial Pangea, present-day American Southwest. *Geological Society of America Bulletin* 127(11-12): 1798-1815. DOI: 10.1130/B31186.1
- Padian, K. 2013. Why study the bone microstructure of fossil tetrapods?, pp. 1-12 in K. Padian and E.-T. Lamm (eds.), *Bone Histology of Fossil Tetrapods*. University of California Press, Berkeley.
- Parker, W.G. and Martz, J.W. 2010. The Late Triassic (Norian) Adamanian–Revueltian tetrapod faunal transition in the Chinle Formation of Petrified Forest National Park, Arizona. *Earth and Environmental Science Transactions of the Royal Society of Edinburgh* 101(3-4): 231-260. DOI: 10.1017/S1755691011020020
- Rinehart, L.F. and Lucas, S.G. 2009. Limb allometry and lateral line groove development indicates terrestrial-to-aquatic lifestyle transition in Metoposauridae (Amphibia: Temnospondyli) [paper no. 96-14]. *Geological Society of America Abstracts with Program* 41(7): 263.

- Rowe, C.M., Loope, D.B., Oglesby, R.J., Van der Voo, R. and Broadwater, C.E. 2007. Inconsistencies between Pangean reconstructions and basic climate controls. *Science* 318(5854): 1284-1286. DOI: 10.1126/science.1146639
- Sanchez, S. and Schoch, R.R. 2013. Bone histology reveals a high environmental and metabolic plasticity as a successful evolutionary strategy in a long-lived homeostatic Triassic temnospondyl. *Evolutionary Biology* 40(4): 627-647. DOI 10.1007/s11692-013-9238-3
- Schoch, R.R. 2014. Life cycles, plasticity and palaeoecology in temnospondyl amphibians. *Palaeontology*, 57(3): 517-529. DOI: 10.1111/pala.12100
- Spielmann, J.A. and Lucas, S.G. 2012. Tetrapod Fauna of the Upper Triassic Redona Formation East-central New Mexico: The Characteristic Assemblage of the Apachean Land-vertebrate Faunachron. *New Mexico Museum of Natural History and Science Bulletin* 55. New Mexico Museum of Natural History and Science, Albuquerque.
- Steiner, M.B. and Lucas, S.G. 2000. Paleomagnetism of the Late Triassic Petrified Forest Formation, Chinle Group, western United States: Further evidence of “large” rotation of the Colorado Plateau. *Journal of Geophysical Research* 105(B11): 25-791.
- Steyer, J.S. 2000. Ontogeny and phylogeny in temnospondyls: a new method of analysis. *Zoological Journal of the Linnean Society* 130(3): 449-467. DOI: 10.1111/j.1096-3642.2000.tb01637.x
- Steyer, J.S., Laurin, M., Castanet, J. and De Ricqlès, A. 2004. First histological and skeletochronological data on temnospondyl growth: palaeoecological and palaeoclimatological implications. *Palaeogeography, Palaeoclimatology, Palaeoecology* 206(3): 193-201. DOI: 10.1016/j.palaeo.2004.01.003
- Sulej, T. 2007. Osteology, variability, and evolution of *Metoposaurus*, a temnospondyl from the Late Triassic of Poland. *Palaeontologia Polonica* 64: 29-139.
- Warren, A. and Snell, N. 1991. The postcranial skeleton of Mesozoic temnospondyl amphibians: a review. *Alcheringa* 15(1): 43-64.
- Werning, S. 2012. The ontogenetic osteohistology of *Tenontosaurus tilletti*. *PLoS ONE* 7(3): e33539. DOI: 10.1371/journal.pone.0033539



- Witzmann, F., Scholz, H. and Ruta, M. 2009. Morphospace occupation of temnospondyl growth series: a geometric morphometric approach. *Alcheringa*, 33(3): 237-255. DOI: 10.1080/03115510903043606
- Witzmann, F. and Soler-Gijón, R. 2010. The bone histology of osteoderms in temnospondyl amphibians and in the chroniosuchian *Bystrowiella*. *Acta Zoologica* 91(1): 96-114. DOI: 10.1111/j.1096-3642.2009.00599.x
- Zanno, L. E., Heckert, A. B., Krzyzanowski, S. E., and Lucas, S. G. 2002. Diminutive metoposaurid skulls from the Upper Triassic Blue Hills (Adamanian: latest Carnian) of Arizona; pp. 121-126 in A.B. Heckert and S.G. Lucas (eds.), *Upper Triassic Stratigraphy and Paleontology*. New Mexico Museum of Natural History and Science Bulletin 21. New Mexico Museum of Natural History and Science, Albuquerque.
- Zeigler, K.E. and Geissman, J.W. 2011. Magnetostratigraphy of the Upper Triassic Chinle Group of New Mexico: Implications for regional and global correlations among Upper Triassic sequences. *Geosphere* 7(3): 802-829. DOI: 10.1130/GES00628.1

## Figure Captions

**Figure 1. Map of PEFO showing localities of sampled specimens.** Localities and associated specimens are as follows: PFV 122 (Blue Mesa Member): PEFO 4826 and PEFO 38726; PFV 040 (Petrified Forest Member): PEFO 38645; PFV 215 (Petrified Forest Member): PEFO 36874, PEFO 16696, and PEFO 35392.

**Figure 2. Stratigraphic column of PEFO showing position of sampled specimens and localities.** Localities and associated specimens are as follows: PFV 122 (Blue Mesa Member): PEFO 4826 and PEFO 38726; PFV 040 (Petrified Forest Member): PEFO 38645; PFV 215 (Petrified Forest Member): PEFO 36874, PEFO 16696, and PEFO 35392.

**Figure 3. Photographs of sampled specimens in anterior and lateral profiles.** (A) PEFO 38726, (B) PEFO 4826, (C) PEFO 38645, (D-E) PEFO PEFO 36874, (F-G) PEFO 35392, (H-J) PEFO 16696. Order of photographed specimens mirrors their listed order in Table 1.

**Figure 4. Microphotographs of the sagittal sections of sampled specimens.** (A) PEFO 36874a, (B) PEFO 16696a, (C) PEFO 4826, (D) PEFO 16696b, (E) PEFO 38645, (F) PEFO 36874b (G) PEFO 35392a, (H) PEFO 16696c, (I) PEFO 35392, (J) PEFO 38726. Scale bars equal to 4 mm.

647 **Figure 5. Microphotographs of the notochordal channel in three small specimens.** (A) PEFO  
648 4826 (B) PEFO 36874a, (C) PEFO 16696a. Scale bars equal to 1 mm.

649 **Figure 6. Microphotographs of the periosteal region in three small specimens.** (A) PEFO  
650 4826 (B) PEFO 36874a, (C) PEFO 16696a, (D) PEFO 16696b. Scale bars equal to 1 mm.

651 **Figure 7. Microphotographs of the dorsal endochondral region in three small specimens.**  
652 (A) PEFO 4826 (B) PEFO 36874a, (C) PEFO 16696a. Scale bars equal to 1 mm.

653 **Figure 8. Microphotograph of the external cortex in large intercentra.** (A) PEFO 38645, (B)  
654 PEFO 35392a, (C) PEFO 16696c, (D) PEFO 38726. Arrows indicate the position of the LAGs in  
655 PEFO 38726. Scale bars equal to 1 mm.

# Figure 1

Map of PEFO showing localities of sampled specimens.

Localities and associated specimens are as follows: PFV 122 (Blue Mesa Member): PEFO 4826 and PEFO 38726; PFV 040 (Petrified Forest Member): PEFO 38645; PFV 215 (Petrified Forest Member): PEFO 36874, PEFO 16696, and PEFO 35392.

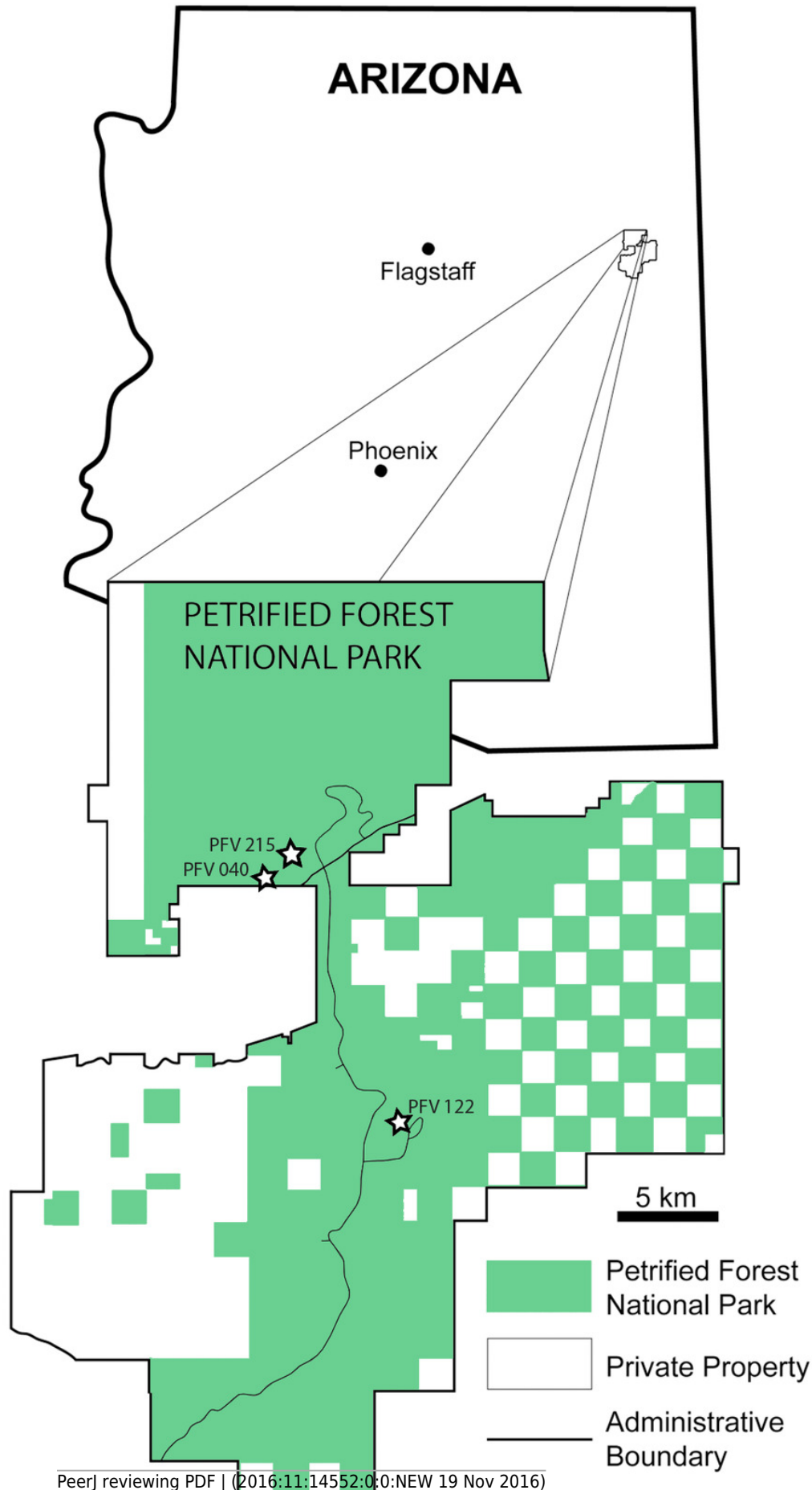


# Figure 2

Stratigraphic column of PEFO showing position of sampled specimens and localities.

Localities and associated specimens are as follows: PFV 122 (Blue Mesa Member): PEFO 4826 and PEFO 38726; PFV 040 (Petrified Forest Member): PEFO 38645; PFV 215 (Petrified Forest Member): PEFO 36874, PEFO 16696, and PEFO 35392.

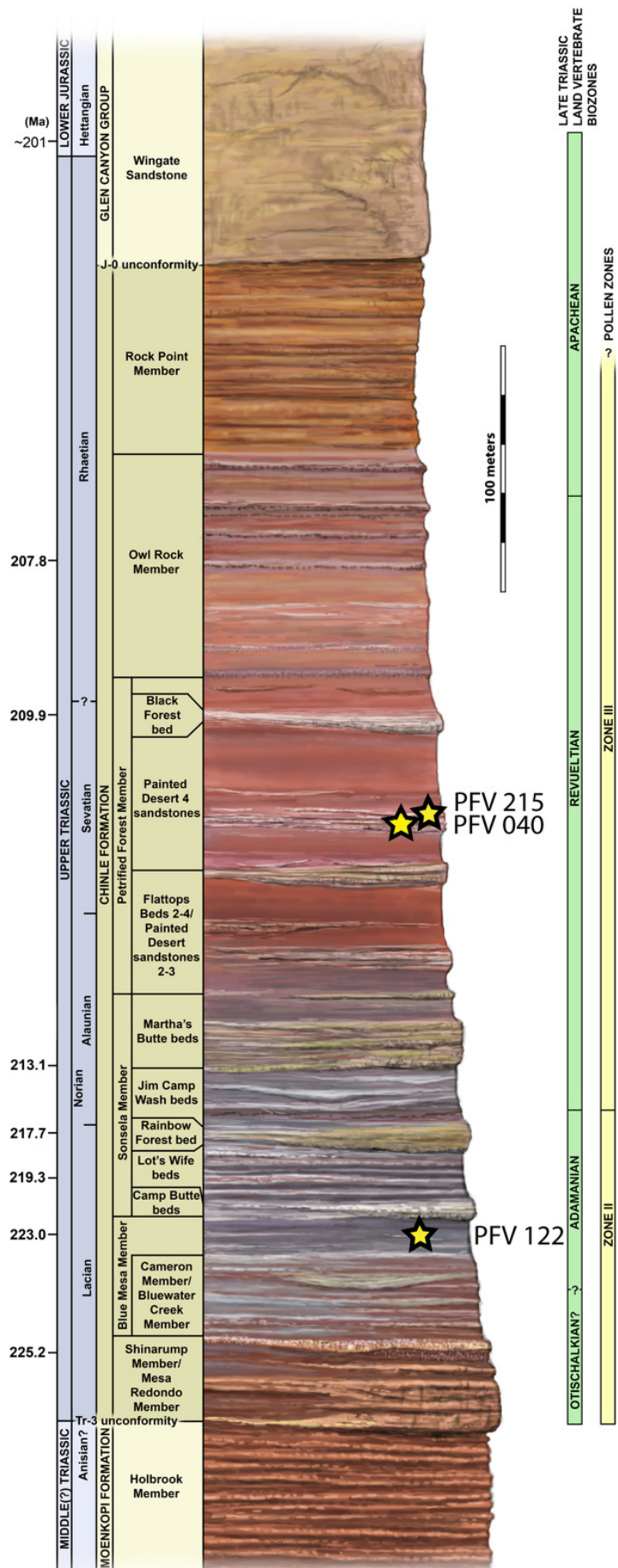
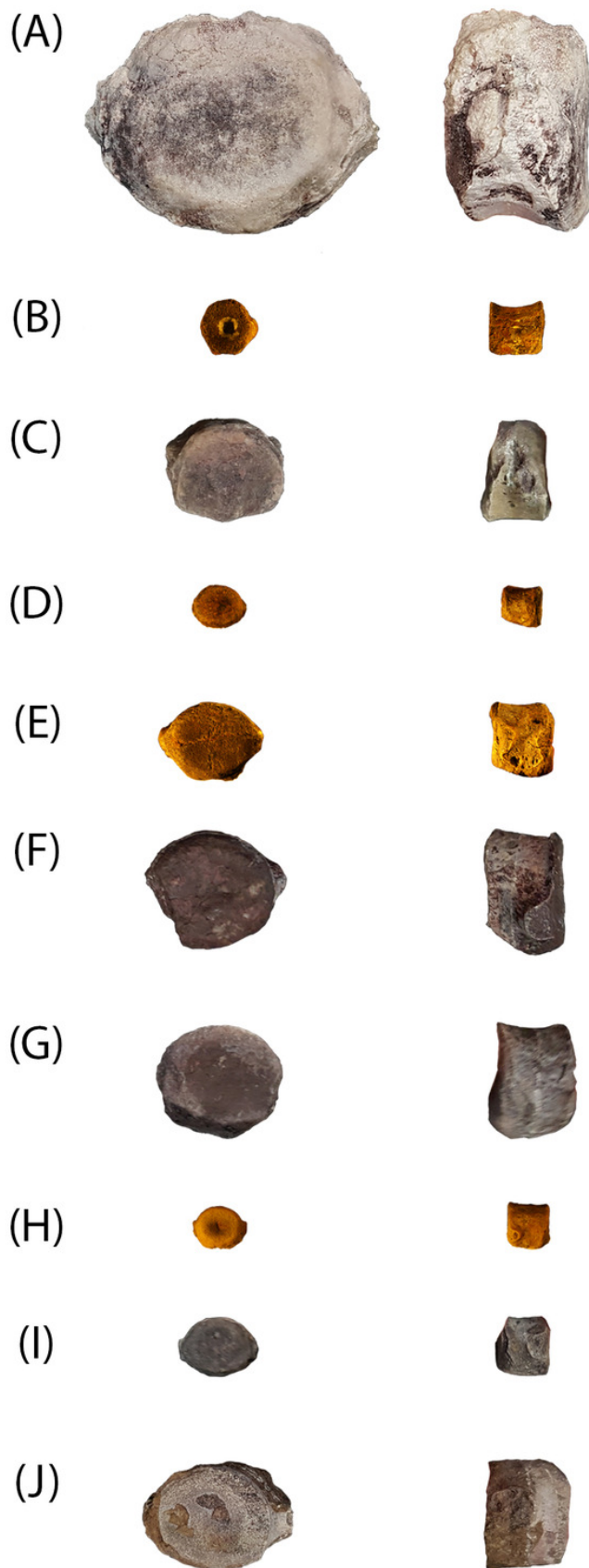


# Figure 3

Photographs of sampled specimens in anterior and lateral profiles.

(A) PEFO 38726, (B) PEFO 4826, (C) PEFO 38645, (D-E) PEFO PEFO 36874, (F-G) PEFO 35392, (H-J) PEFO 16696. Order of photographed specimens mirrors their listed order in Table 1.



2 cm



# Figure 4

Microphotographs of the sagittal sections of sampled specimens.

(A) PEFO 36874a, (B) PEFO 16696a, (C) PEFO 4826, (D) PEFO 16696b, (E) PEFO 38645, (F) PEFO 36874b (G) PEFO 35392a, (H) PEFO 16696c, (I) PEFO 35392, (J) PEFO 38726. Scale bars equal to 4 mm.

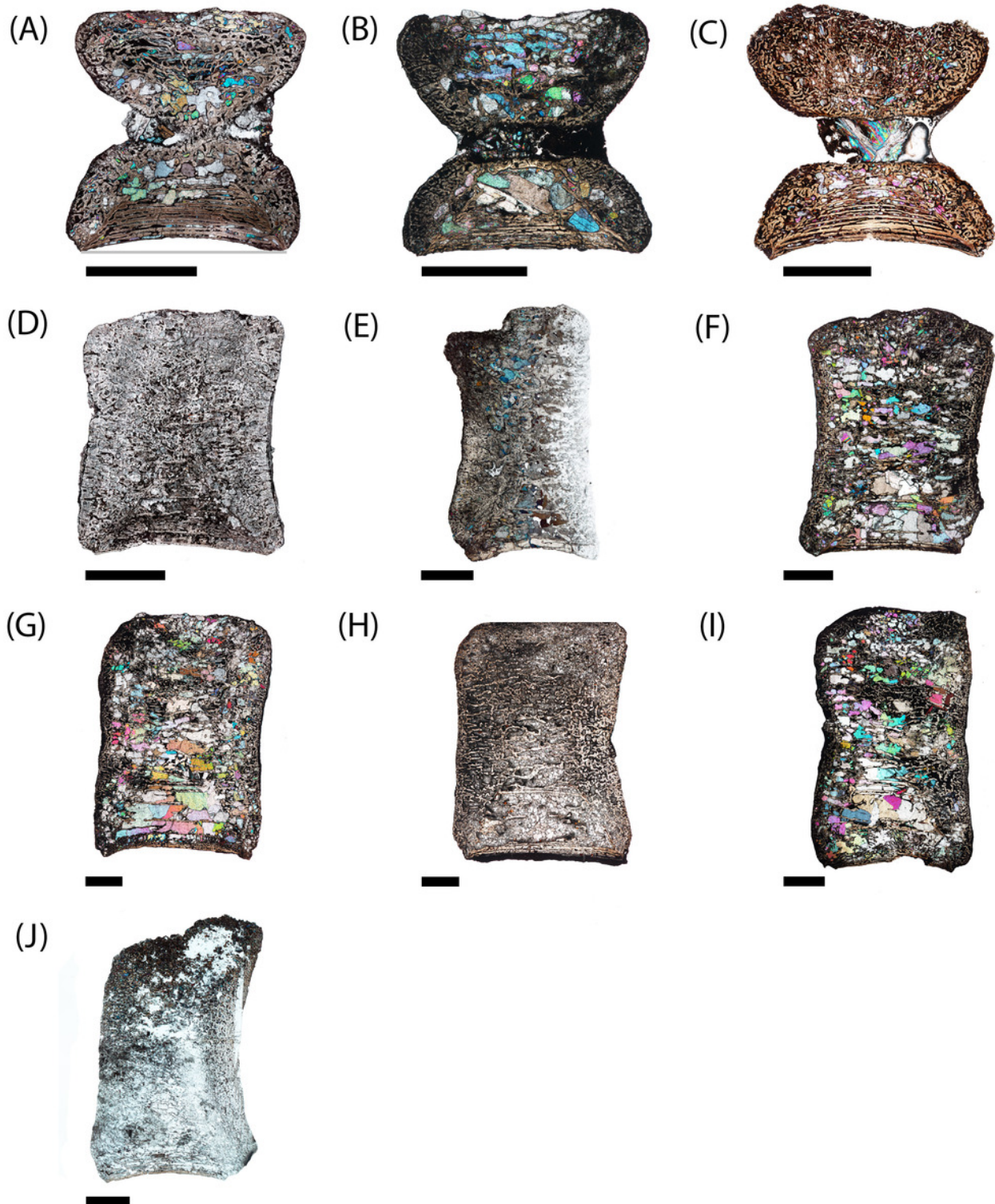


# Figure 5

Microphotographs of the notochordal channel in three small specimens.

(A) PEFO 4826 (B) PEFO 36874a, (C) PEFO 16696a. Scale bars equal to 1 mm.



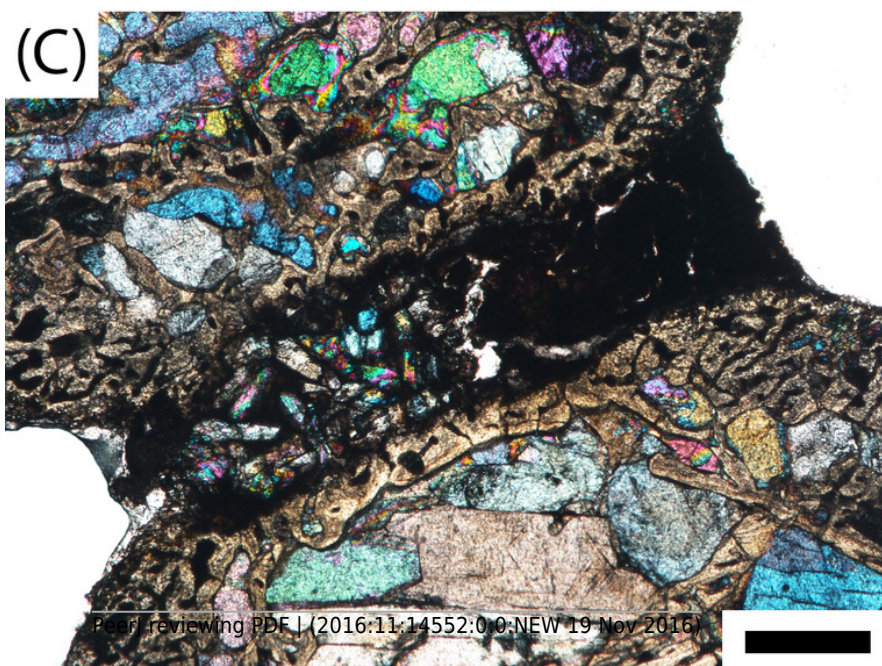
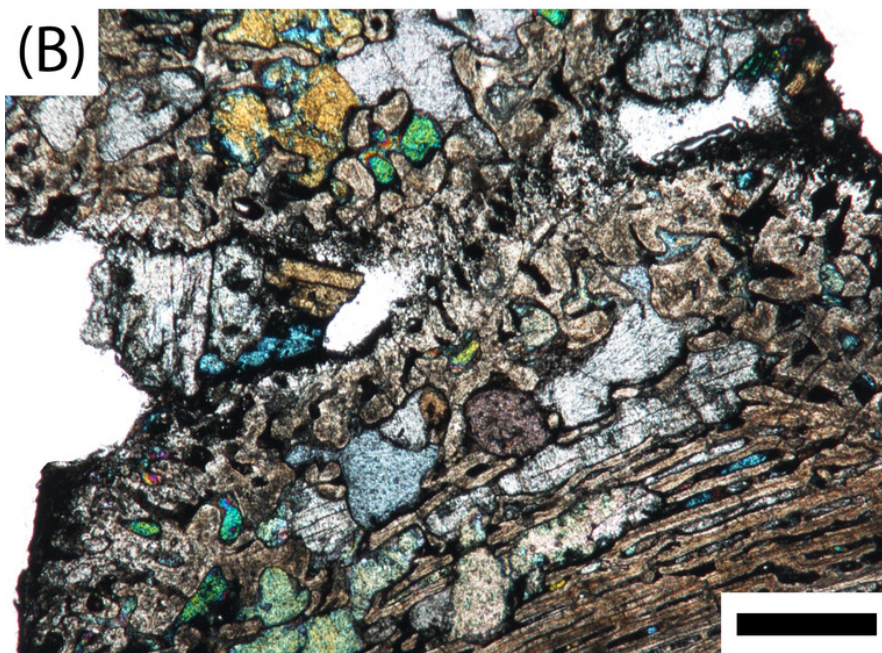
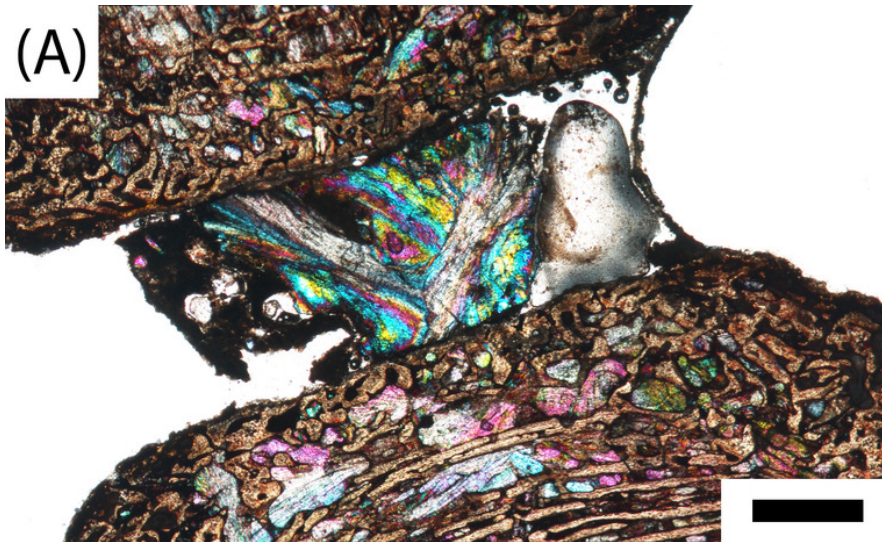




# Figure 6

Microphotographs of the periosteal region in three small specimens.

(A) PEFO 4826 (B) PEFO 36874a, (C) PEFO 16696a, (D) PEFO 16696b. Scale bars equal to 1 mm.

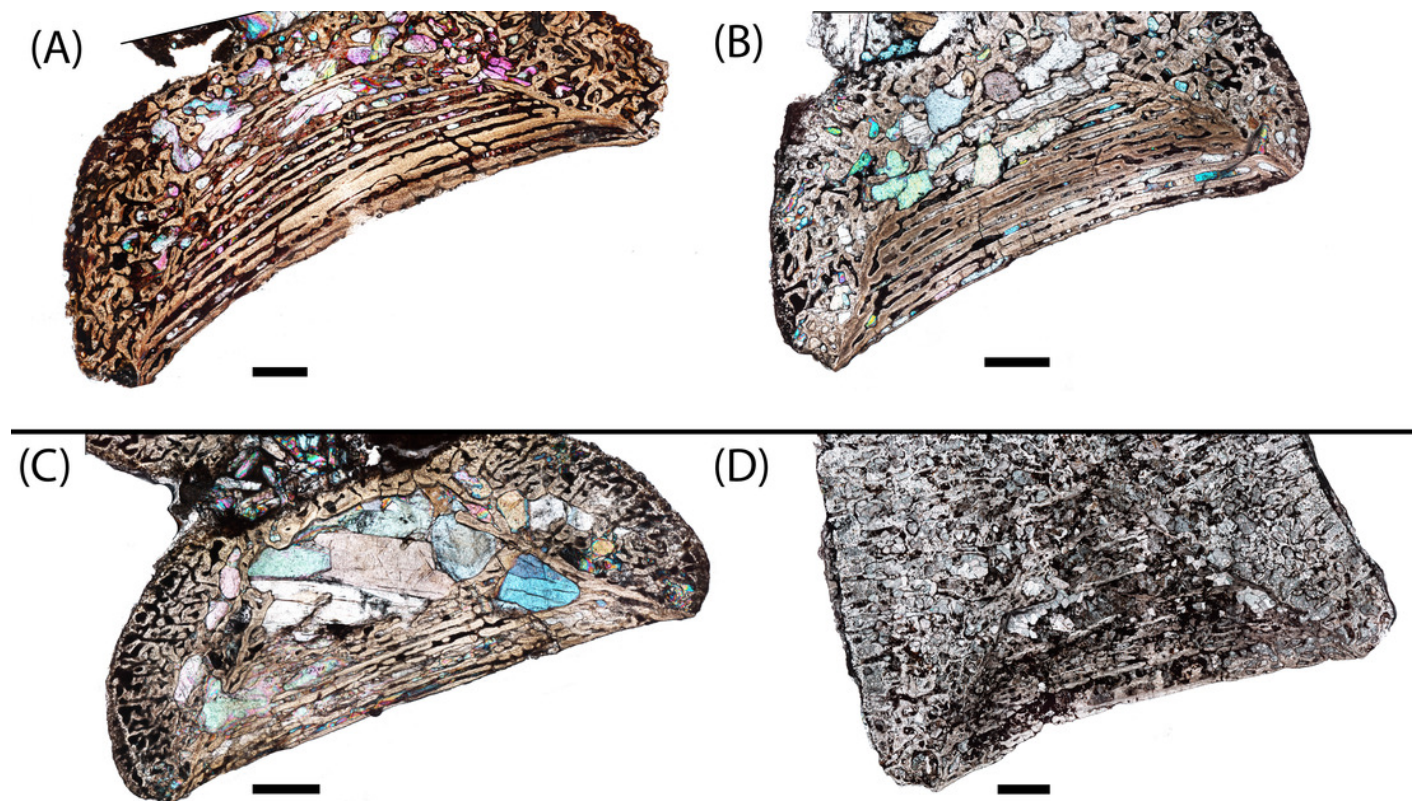


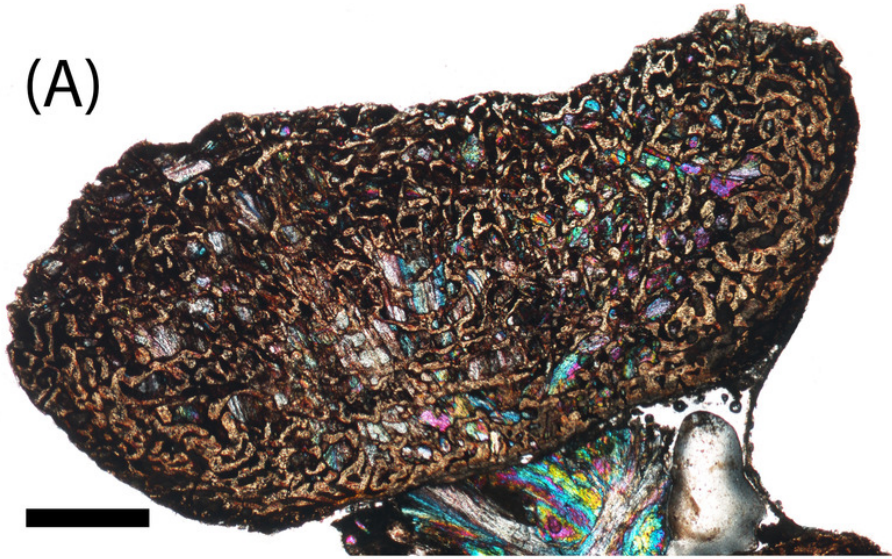
# Figure 7

Microphotographs of the dorsal endochondral region in three small specimens.

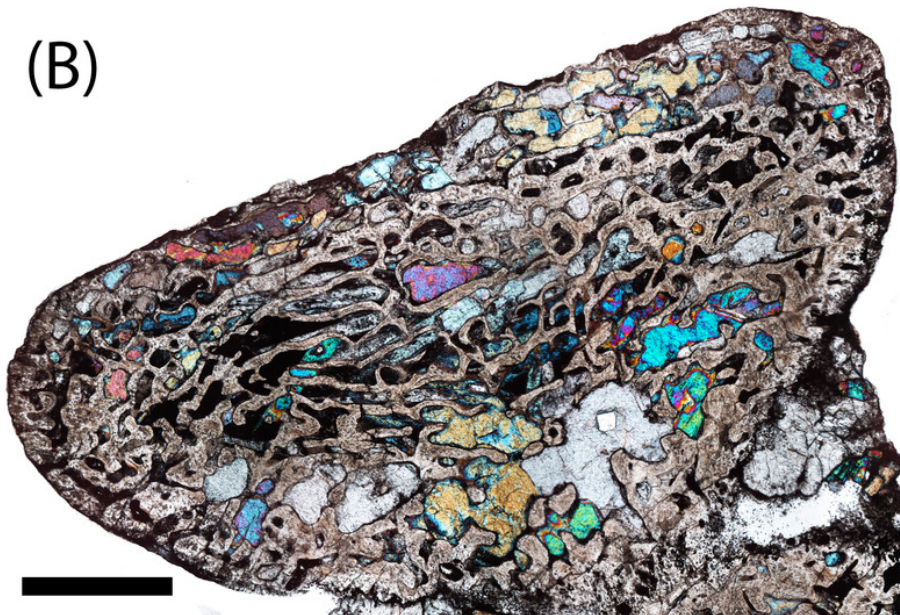
(A) PEFO 4826 (B) PEFO 36874a, (C) PEFO 16696a. Scale bars equal to 1 mm.



(A)



(B)



(C)

1 mm

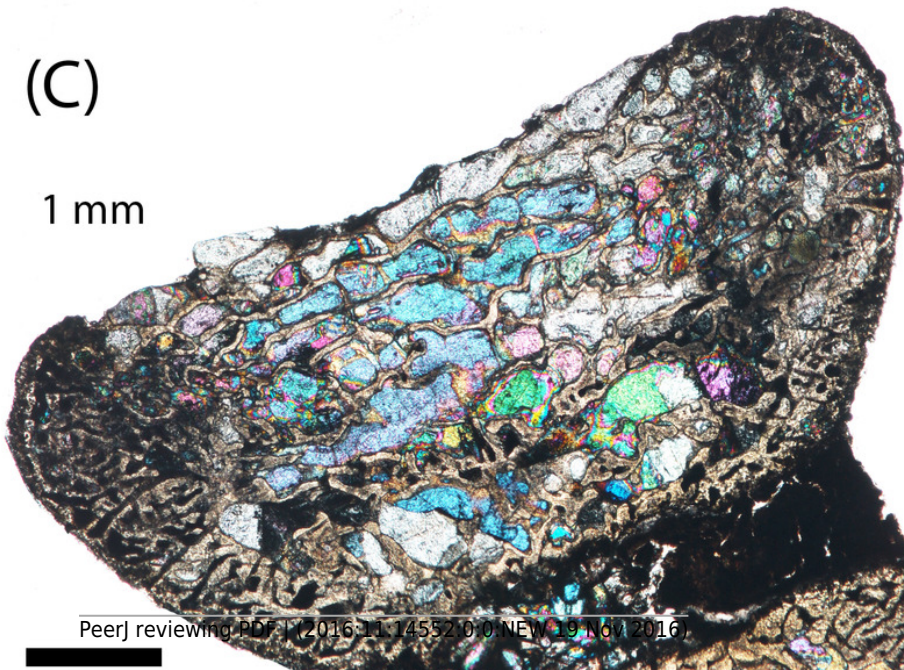




# Figure 8

Microphotograph of the external cortex in large intercentra.

(A) PEFO 38645, (B) PEFO 35392a, (C) PEFO 16696c, (D) PEFO 38726. Arrows indicate the position of the LAGs in PEFO 38726. Scale bars equal to 1 mm.

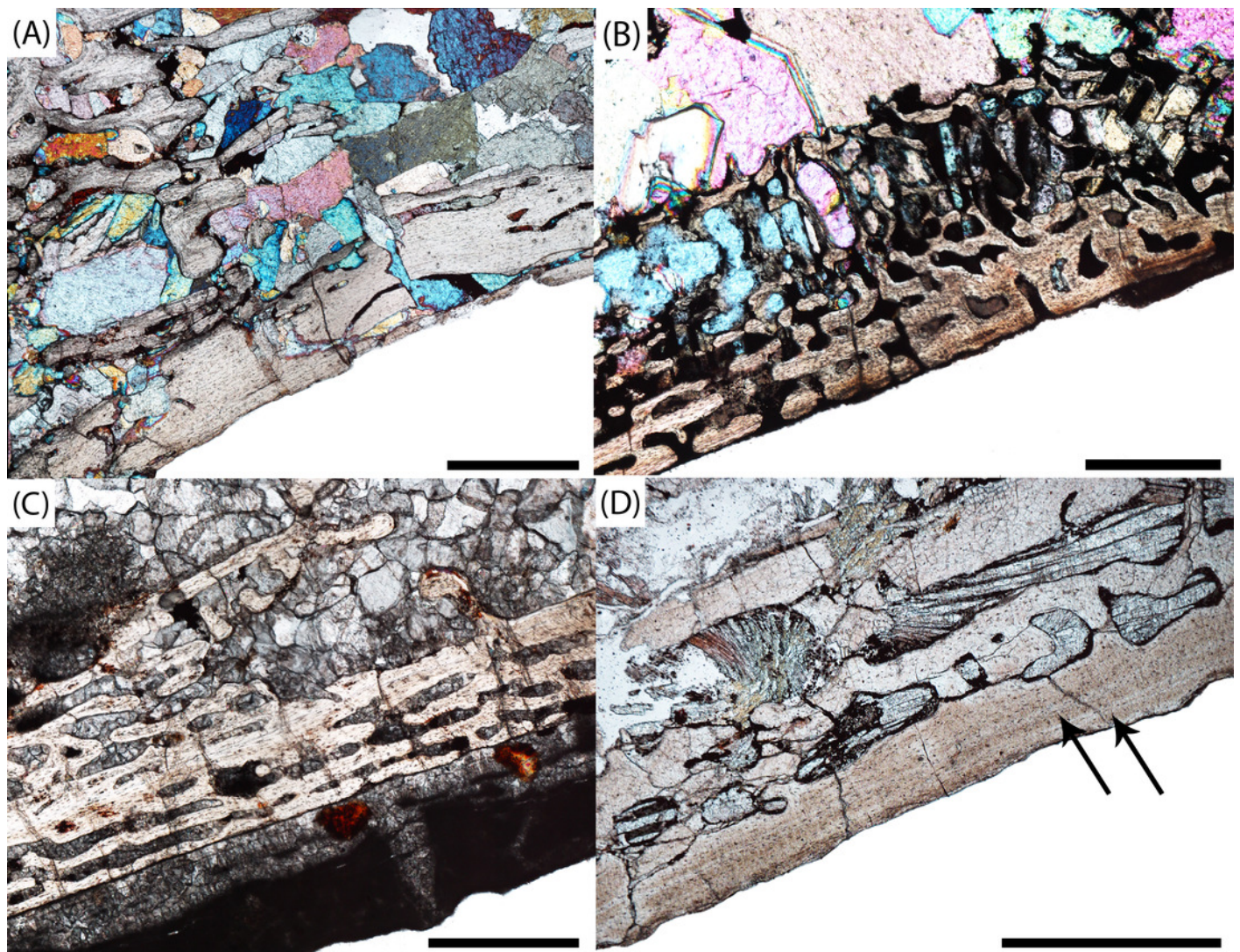




# **Table 1**(on next page)

Summary of intercentra analyzed in this experiment.

For specimens with multiple elements, the listed order reflects their order by size, from smallest to largest. Letter assignments for multi-element specimens were created for the purpose of this publication to facilitate their references throughout the text. Measurements were performed in the same manner as in Konietzko-Meier, Bodzioch, & Sander (2012), where length is in the anteroposterior axis, width is in the mediolateral axis, and height is in the dorsoventral axis. *Geologic member abbreviations: BMM – Blue Mesa Member; PFM – Petrified Forest Member.*

**Table 1. Summary of intercentra analyzed in this experiment.** For specimens with multiple elements, the listed order reflects their order by size, from smallest to largest. Letter assignments for multi-element specimens were created for the purpose of this publication to facilitate their references throughout the text. Measurements were performed in the same manner as in Konietzko-Meier, Bodzioch, & Sander (2012), where length is in the anteroposterior axis, width is in the mediolateral axis, and height is in the dorsoventral axis. *Geologic member abbreviations: BMM – Blue Mesa Member; PFM – Petrified Forest Member.*

Specimen number	Estimated position	Cutting plane	Length (mm)	Width (mm)	Height (mm)	W:L	Geologic member
PEFO 38726	anterior dorsal	sagittal	22.98	55.32	46.91	2.40	BMM
PEFO 4826	dorsal	sagittal	10.25	10.55	12.71	1.03	BMM
PEFO 38645	presacral	sagittal	10.99	21.90	19.32	1.99	PFM
PEFO 36874a	dorsal	sagittal	7.65	10.72	8.85	1.40	PFM
PEFO 36874b	perisacral	sagittal	11.85	19.63	17.25	1.65	PFM
PEFO 35392	mid-dorsal	sagittal	15.43	28.27	25.74	1.83	PFM
PEFO 35392b	anterior dorsal	sagittal	15.37	25.89	24.72	1.68	PFM
PEFO 16696a	pre-sacral	sagittal	8.22	10.22	9.09	1.24	PFM
PEFO 16696b	mid-dorsal	sagittal	9.52	15.96	12.11	1.67	PFM
PEFO 16696c	mid-dorsal	sagittal	16.60	26.83	16.13	1.61	PFM

## Table 2 (on next page)

Summary of major histological landmarks identified in the sampled specimens.

For specimens with multiple elements, the listed order reflects their order by size, from smallest to largest. Dots indicate the presence of the structure in specimens.

- 1 **Table 2. Summary of major histological landmarks identified in the sampled specimens.** For
- 2 specimens with multiple elements, the listed order reflects their order by size, from smallest to largest.
- 3 Dots indicate the presence of the structure in specimens.

Specimen ID	Periosteal bone	External cortex	LAGs	HOS
PEFO 38726	•	•	•	4
PEFO 4826	•			2
PEFO 38645	•	•		3
PEFO 36874a	•			2
PEFO 36874b	•	•		3
PEFO 35392	•	•		3
PEFO 35392b	•	•		3
PEFO 16696a	•			2
PEFO 16696b	•			2
PEFO 16696c	•	•		3